Journal of Magnetism and Magnetic Materials 406 (2016) 110–117

Contents lists available at ScienceDirect

Journal of Magnetism and Magnetic Materials

journal homepage: www.elsevier.com/locate/jmmm

Current Perspectives

Magnetic and dielectric properties of Co doped nano crystalline Li ferrites by auto combustion method

G. Aravind [a], M. Raghasudha [b,*], D. Ravinder [a], R. Vijaya Kumar [c]

[a] Department of Physics, Osmania University, Hyderabad 500007, Telangana State, India
[b] Department of Chemistry, Osmania University, Hyderabad 500007, Telangana State, India
[c] School of Physics, University of Hyderabad, 500046 Telangana State, India

ARTICLE INFO

Article history:
Received 15 March 2015
Received in revised form
25 October 2015
Accepted 21 December 2015
Available online 29 December 2015

Keywords:
Citrate-gel method
X-ray diffraction studies
Field emission scanning electron microscopy
Vibrating sample magnetometer
Hysteresis loop
Dielectric parameters

ABSTRACT

The ultra fine particles of the cobalt substituted lithium ferrites with the formula $[Li_{0.5}Fe_{0.5}]_{1-x}Co_xFe_2O_4$ ($0.0 \le x \le 1.0$) were synthesized by low temperature citrate-gel auto combustion method. Structural characterization of the samples was carried out using XRD studies and FESEM (Field Emission Scanning Electron Microscopy) analysis. XRD studies confirms the formation of single phased spinel structure with crystallite size in the range of 36–43 nm. The *M–H* loops have been traced using Vibrating Sample Magnetometer (VSM) for all the compositions at room temperature and hysteresis parameters were evaluated. The hysteresis loops of the prepared samples show clear saturation at an applied field of $\pm$ 20 k Oe and the loops were highly symmetric in nature. The dielectric parameters such as dielectric constant (ε'), dielectric loss tangent ($\tan\delta$) of the samples were studied as a function of frequency in the range of 20 Hz to 2 MHz at room temperature using LCR Meter. The dielectric constant and loss tangent of the samples show a normal dielectric behavior with frequency which reveals that the dispersion is due to the Maxwell-Wagner type interfacial polarization and hopping of electrons between the Fe^{2+} and Fe^{3+} ions.

1. Introduction

Nano crystalline spinel ferrites have been the subject of interest for many researchers due to their enhanced optical, structural, electrical and magnetic properties, when compared with their bulk counterparts. These properties of nano particles make them desirable for a variety of applications such as in electronics, optical devices, magnetic storage devices, coolants, MLCI applications [1]. Nano crystalline magnetic ferrites are also used as permanent magnets in many devices instead of pure metals because of their high resistivity, low eddy current loss, low magnetic loss and low cost. According to the crystal structure, spinel ferrites possess AB_2O_4 type crystal structure with tetrahedral (A) sites and octahedral (B) sites. They show various magnetic properties depending on their composition and cation distribution on the two sites. Various metal cations occupied in tetrahedral site and octahedral site tune the magnetic and dielectric properties of ferrites. Depending on occupancy of tetrahedral and octahedral sites, ferrites exhibit ferri-magnetic, anti-ferromagnetic, spin clusters and paramagnetic behavior [2]. Hence, many researchers have focused on investigating the effect of transition metal ion doping in the spinel ferrite crystal lattice.

Various properties of ferrites suchas magnetic and electrical properties depend on their microstructure which is determined by various factors. They are quality of the raw materials used, sintering temperature, sintering time and the materials composition. The microstructure of the material developed during sintering is determined by particle size, shape, porosity, agglomeration, chemical and phase composition which are closely related to the processing technique [3].

Lithium and substituted lithium ferrites are promising materials for the microwave device applications since they are less sensitive to the stress and possess high Curie temperature (T_c). Lithium ferrites are used in microwave devices such as isolators, circulators, gyrators and phase shifters. They play a vital role in microwave latching devices, magnetic switching circuits. They can also be used as cathode materials in lithium batteries. Many researchers have reported the effect of magnetic and non-magnetic substitutions in lithium ferrites on their various properties [4–5].

The applications of lithium ferrites were restricted due to the difficulties experienced in sintering the prepared samples at the high temperatures. The irreversible loss of lithium and oxygen during sintering was the main cause that made lithium ferrites difficult to synthesize [6]. Spinel Ferrites can be synthesized by

* Corresponding author.
E-mail address: raghasudha_m@yahoo.co.in (M. Raghasudha).

http://dx.doi.org/10.1016/j.jmmm.2015.12.087
0304-8853/

various techniques viz., standard Ceramic method [7], Chemical co-precipitation method [8], Solid state reaction [9], Hydrothermal process [10], Micro-emulsion method [11] and sol–gel method [12].

The ceramic method has some inherent drawbacks such as, Poor compositional control, Chemical inhomogeneity, Coarse particle size, Introduction of impurities during grinding and requires high temperature (>1000 °C). By using various wet chemical routes such as co-precipitation, sol–gel, freeze drying, spray drying etc. the particle size can be brought down at lower temperature compared to ceramic technique. These wet chemical methods are reproducible, low cost and requires low temperature. In the recent years, sol–gel method is the most effective method for the synthesis of pure and homogeneous nanoparticles at relatively low temperatures due to its potential to produce relatively large quantities of final product at low cost as compared to other chemical processes [13].

In the sol–gel auto combustion reaction method, if the organic fuel used is Citric acid, the method is called citrate-gel auto combustion method. In this method the citrate precursors decompose at temperature less than 500 °C and hence it has been possible to prepare spinel ferrites at relatively low temperatures by this method [14].

Hence, it is clear that the citrate sol–gel auto combustion method provides an easy alternative for the synthesis of lithium nano crystalline ferrites at low temperature sintering itself [15].

The magnetization studies were useful in understanding the arrangement of spins and the distribution of magnetic cations in the sub-lattice. It is a well known fact that the properties of the spinel ferrites were also sensitive to the presence of doped cations and amount of doping. The substitution of small amount of impurities changes the electrical and magnetic properties of ferrites. The modifications in the properties of lithium ferrites by the substitution of different ions have been studied by various researchers [16–17]. The authors have assumed that the substitution of non-magnetic lithium ion with magnetic cobalt ion may result in improvement of their magnetic and electrical properties. Moreover, there are very few reports on the synthesis and properties of single phased cobalt substituted lithium nano crystalline ferrite particles by the citrate gel auto-combustion method.

The present study reports the synthesis of nano crystalline cobalt substituted lithium ferrites using low temperature citrate-gel auto combustion method. Characterization, magnetic and dielectric properties of the prepared ferrites were also discussed in the present article.

2. Experimental technique

The properties of ferrites are profoundly influenced by the preparation conditions. Nano crystalline cobalt substituted lithium ferrites with the chemical formula $[Li_{0.5}Fe_{0.5}]_{1-x}Co_xFe_2O_4$ ($0.0 \le x \le 1.0$) were prepared by low temperature auto-combustion method. The synthesized ferrite samples were characterized by X-ray diffraction studies using Philips X-ray diffractometer (3710). The surface morphology of the samples was studied by Field Emission Scanning Electron Microscope (FE-SEM model-JSM-7610F).

The magnetic properties of the synthesized samples were measured by using Vibrating Sample Magnetometer (VSM, Model-155) and dielectric properties were measured by using Agilent E4980 LCR meter.

The starting materials used for the synthesis of Li–Co ferrites under investigation are Ferric nitrate–$Fe(NO_3)_2 9H_2O$, Cobalt nitrate–$Co(NO_3)_2 6H_2O$, Lithium nitrate–$LiNO_3$, Citric acid $C_6H_8O_7.H_2O$ and Ammonia solution–NH_3. All the raw materials used are 99.0% pure (Sigma Aldrich Company) and are used without any further purification.

Li–Co ferrite samples with desired composition were synthesized using citrate-gel auto combustion method. The detailed flow chart for this method was explained in our earlier publication [18–19]. Calculated quantities of above mentioned metal nitrates were dissolved in double distilled water and required amount of aqueous citric acid solution was added that acts as orgamic fuel. The mixture was placed on a magnetic stirrer for thorough stirring to get a homogeneous solution. Ammonia solution was added to this nitrate-citrate mixture to adjust the pH to 7. The mixed solution was heated on a magnetic hot plate at about 100 °C with uniform stirring and was evaporated to obtain a highly viscous gel described as precursor. The resultant gel was further heated on a hot plate maintained in a temperature range of 180–200 °C. Finally, when all water molecules were removed from the mixture, the viscous gel began rising with sodt mass. The gel gave a fast flameless self ignited combustion reaction with the evolution of large amounts of gaseous products. It started in the hot portion of the beaker and propagated from the bottom to the top like a volcanic eruption. The reaction was completed in a minute giving rise to dark gray product. The synthesized powders were sintered at 500 °C for 4 h in air at a slow heating rate of 5 °C/min and then furnace was cooled to room temperature. The cooled samples were ground using mortar and pestle for getting fine powdered samples.

The resulting samples were used for structural characterization using x-ray diffraction studies. Part of the prepared samples was x-ray examined by X-ray diffractometer using Cu-K_α radiation of wavelength (λ) 1.5405 Å with a scanning step increment of 0.02 and scanning rate of 2 °/min. The x-ray generator was operated at 40 kV and 30 mA. A specially designed silicon sample was used as the instrumental standard. The crystallite size (D) of the prepared samples has been estimated from the full-width half maxima (FWHM) of the strongest reflection of the plane (311) using Debye Scherer's formula as mentioned below

$$D = \frac{0.91\lambda}{\beta \cos\theta} \tag{1}$$

where β is the full width at half maximum and θ is the diffraction angle.

The disc shaped pellets of the ferrite samples with 13 mm diameter and 2 mm thickness were prepared by applying a pressure about 39.23×10^3 Pa. The measured density 'ρ_m' was calculated by the following expression [20],

$$\rho_m = \frac{M}{V} \tag{2}$$

where 'M' is the mass of the pellet that was determined using a digital balance, and 'V' is the volume of the pellet.

The specific surface area of the prepared samples was calculated from the following relation [21].

$$S = \frac{6000}{D\rho_m} \tag{3}$$

where D is the crystallite size and the ρ_m is the measured density.

The FE scanning electron microscope (FE-SEM) is a very useful tool for high-resolution surface imaging in the fields of nanomaterials science. Electron microscopes use a beam of highly energetic electrons to probe objects on a very fine scale. In standard electron microscopes, electrons are mostly generated by "heating" a tungsten filament (electron gun). On the other hand, in a field emission (FE) electron microscope, no heating but a so-called "cold" source is employed. The FE source reasonably combines with scanning electron microscopes (SEMs) whose development

has been supported by advances in secondary electron detector technology. The electron beam produced by the FE source is about 1000 times smaller than that in a standard microscope with a thermal electron gun. Hence, the image quality of the prepared samples was markedly improved [22].

The magnetic properties of the prepared Li–Co ferrite samples as a function of composition at 300 K were determined using a Vibrating Sample Magnetometer (VSM) at a maximum field of 20 kOe. Various magnetic parameters were measured from the hysteresis loops obtained from the VSM measurements.

The experimental magnetic moment per formula unit m_{exp} expressed in Bohr Magneton (μ_B) can be calculated using the following formula [23].

$$m_{exp} = \frac{M_w M_s}{5585} \tag{4}$$

where M_w is the molecular weight of the sample and M_s is the saturation magnetization in emu/g.

The magnetic anisotropic constant (K) can be related to the saturation magnetization (M_s) and magnetic coercivity (H_c) [24] as,

$$K = \frac{M_s H_c}{0.96} \tag{5}$$

To measure the dielectric properties, samples should be in the form of pellet, and these pellets were silver pasted for good ohmic contact, calcinated at 500 °C for 4 h at a heating rate of 4 °C/min. Using LCR meter, capacitance (c) and tan δ (loss tangent) of the pellets were measured directly from the instrument. By using this data, dielectric constant (ε') of the prepared samples can be calculated using the following formula [25].

$$\text{Real part of dielectric constant} = \varepsilon' = \frac{cd}{A\varepsilon_0} \tag{6}$$

$$\text{Imaginary part of dielectric constant} = \varepsilon'' = \varepsilon' \tan\delta \tag{7}$$

Where 'c' is the capacitance, 'd' is the thickness and 'A' is the area of cross section of the pellet, ε_0 is the permittivity of free space. From these values, one can analyze the variation of dielectric constant (ε') and dielectric loss tangent (tan δ) with respect to frequency and composition.

3. Results and discussions

3.1. XRD studies

The X-ray diffraction analysis is a powerful non-invasive technique for characterizing crystal structure of the materials. Thus, in order to investigate the phase formation and micro structure, the XRD analysis was carried out on the synthesized samples. X-ray diffraction pattern of the prepared samples was shown in Fig. 1.

All Bragg's reflections have been indexed as (111), (220), (311), (400), (511) and (440) which confirmed the formation of well-defined single phased cubic spinel structure that belongs to the space group Fd3m with JCPDS card number 00-013-0207 without any impurity peak. The strongest reflection was observed from the (311) plane that indicates the spinel phase. Crystallite size and specific surface area of the nano crystalline Li–Co ferrite samples were calculated using the relations (1) and (2) and summarized in the Table 1.

From the table, it is observed that the average crystallite size of the prepared samples was in the range of 36–43 nm and specific surface area of the prepared samples was in the range of 31–36 m^2/gm which shows the nano crystalline nature of the prepared samples. The specific surface area of the prepared ferrites

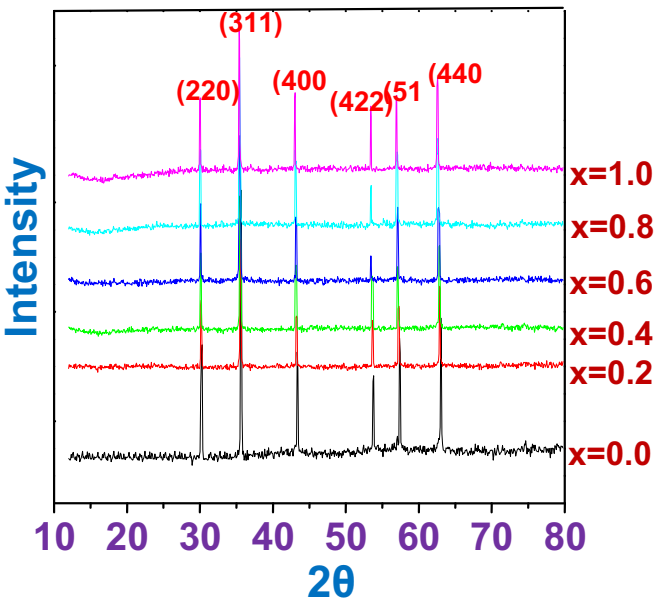

Fig. 1. XRD pattern of $[Li_{0.5}Fe_{0.5}]_{1-x}Co_xFe_2O_4$ ferrites with x=0.0–1.0.

Table 1
Crystallite size, Surface area of the prepared nano crystalline Li–Co ferrites.

Composition	Crystallite size (*D*) (nm)	Average grain size (nm) from FESEM micrograph	Surface area *S* (m^2/gm)
$Li_{0.5}Fe_{2.5}O_4$	41.90	78	33.45
$Li_{0.4}Co_{0.2}Fe_{2.4}O_4$	43.01	85	31.99
$Li_{0.3}Co_{0.4}Fe_{2.3}O_4$	38.44	79	35.63
$Li_{0.2}Co_{0.6}Fe_{2.2}O_4$	37.57	87	36.05
$Li_{0.1}Co_{0.8}Fe_{2.1}O_4$	37.06	84	35.58
$CoFe_2O_4$	36.90	86	34.81

is the aggregation of the areas of the exposed surfaces of the ferrite particles present per unit mass. Crystallite size and the surface area are inversely proportional to each other and is evident from the Table 1. Lesser the crystallite size larger is the surface area of the ferrites which results in the improvement of their properties.

3.2. FE-SEM analysis

The structural morphology of prepared ferrite samples was studied using FE-SEM. The FE-SEM images of the samples were shown in Fig. 2. The average particle size of all the ferrite compositions calculated from FESEM images was in the range of 78–87 nm as depicted in Table 1. It is clear that the average grain size of the various ferrite compositions obtained from FESEM is larger than the crystallite size of the samples as calculated using XRD analysis (Table 2). This fact suggests that each grain is the resultant of agglomeration of number of nanocrystals. The micrographs show the agglomerated grainy structure with clusters of fine particles clinging together. The morphology of surface is almost uniform and regular having cubical to nearly spherical shaped particles. Such morphology of the samples demonstrates the fine particle nature.

3.3. Magnetic measurements

The room temperature magnetization measurements were carried out using Vibrating Sample Magnetometer. For the magnetic measurements, the ferrite samples were made in the form of pellets and were subjected to calcination at 500 °C for 4 h at a

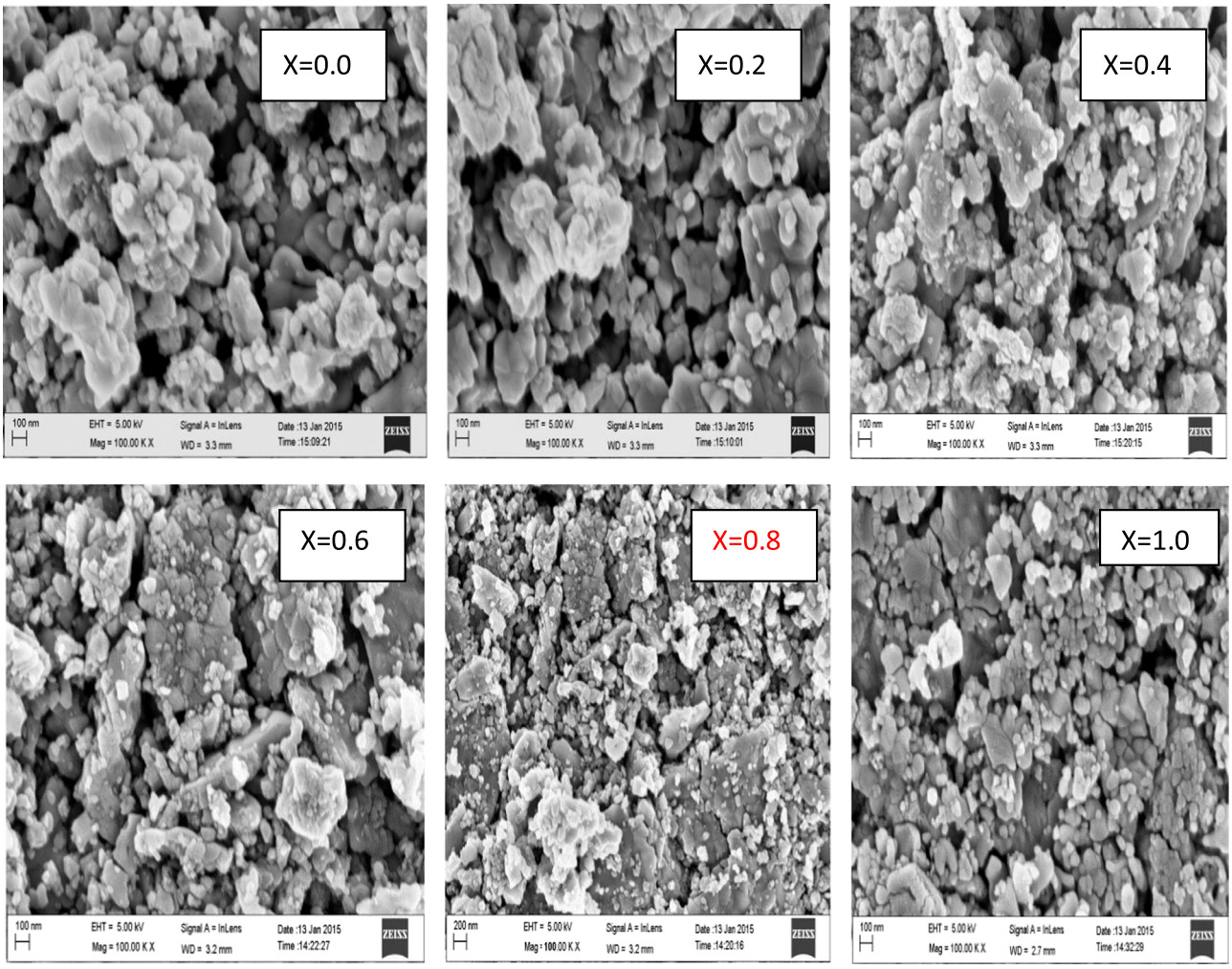

Fig. 2. FE-SEM images of $[Li_{0.5}Fe_{0.5}]_{1-x}Co_xFe_2O_4$ ferrites with x=0.0 to 1.0.

heating rate of 4 °C/min. Hysteresis loops obtained from VSM for all the compositions of Li–Co ferrites were shown in Fig. 3 which show the dependence of Magnetization values (M) on the applied magnetic field (H).

Various magnetic parameters measured from the hysteresis loops are Saturation Magnetization – M_s (Maximum value of magnetization), Remanance Magnetization – M_r (Magnetization at Zero field), Coercivity – H_c (magnetic field required to reduce the magnetization of that material to zero after the magnetization of the sample has been driven to saturation). These Magnetic parameters are used to exemplify the magnetic properties of prepared ferrite materials. The measured magnetic parameters (M_s, M_r and H_c)for the synthesized samples under the applied magnetic field (H) are summarized in Table 2. The measured values show a clear hysteresis loop behavior.

From the figure, one can observe that pure lithium ferrite ($x=0.0$) with least squareness ratio was the soft ferrite and pure cobalt ferrite ($x=1.0$) with maximum squareness ratio was the hard ferrite. Hence, by substituting cobalt in the lithium ferrite, the system changes from soft ferrite into hard ferrite.

The shape and width of the hysteresis loop is influenced by several factors including chemical composition, fabrication method, sintering temperature/time and grain size etc. [new Ref. [15]] [26]. From the figures it is evident that with increase in the cobalt composition in the ferrite system the width of hysteresis loop has increased. This indicates that a very soft magnetic material has changed to hard magnetic material with the introduction of cobalt content in the ferrite system. In spinel ferrites, the magnetic moment of the A-site and B-site were aligned anti-parallel to each other and shows ferri-magnetism with a magnetization M (M_B– M_A).

Table 2
Magnetic parameters (μ_B, K, M_s, H_c and M_r, S) of the prepared nano crystalline Li–Co samples.

Composition	Molecular weight (gm)	Magnetic moment (μ_B)	Anisotropic constant (K) (erg/Oe)	Saturation Magnetization M_s (emu/gm)	Coercivity H_c (Oe)	Remanent magnetization M_r(emu/gm)	Squareness ratio (S)
$Li_{0.5}Fe_{2.5}O_4$	207.079	2.073	8731	55.93	153	15.15	0.270
$Li_{0.4}Co_{0.2}Fe_{2.4}O_4$	212.587	2.219	52,826	58.30	888	25.20	0.449
$Li_{0.3}Co_{0.4}Fe_{2.3}O_4$	218.095	2.369	26,253	60.68	424	30.08	0.495
$Li_{0.2}Co_{0.6}Fe_{2.2}O_4$	223.603	2.497	88,364	62.39	1388	32.34	0.485
$Li_{0.1}Co_{0.8}Fe_{2.1}O_4$	229.111	2.801	107,521	68.29	1543	34.36	0.503
$CoFe_2O_4$	234.619	2.387	121,742	56.84	2099	31.15	0.548

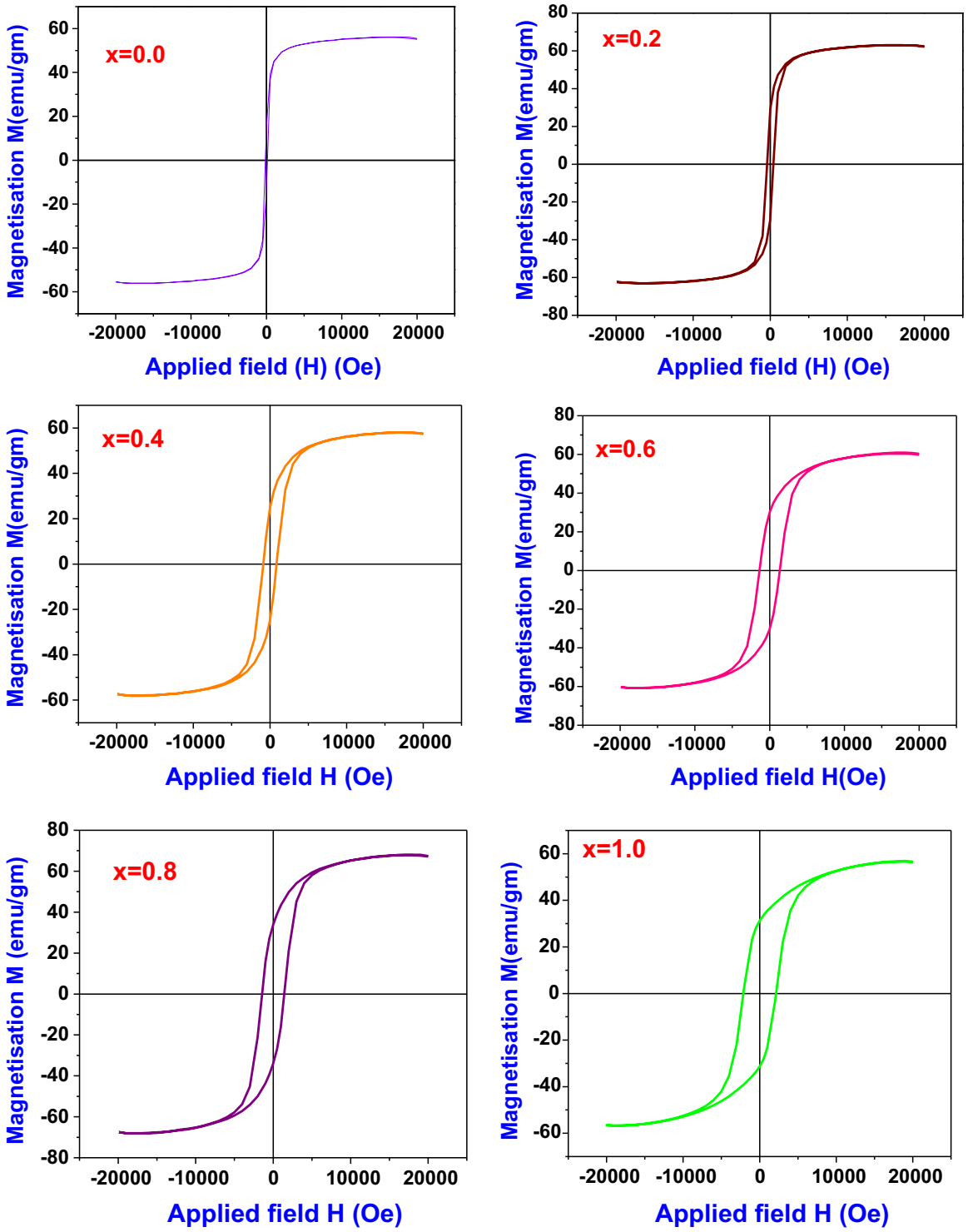

Fig. 3. Hysteresis loops for $[Li_{0.5}Fe_{0.5}]_{1-x}Co_xFe_2O_4$ ferrites with $x=0.0$–1.0.

From measured values one can conclude that in nano crystalline Li–Co ferrites, saturation magnetization (M_s) and remanent magnetization (M_r) values were observed to be increasing with increase in the Co doping until $x \leq 0.8$ beyond which a decrease in the value was observed and is evident from Fig. 4. This observed fact can be explained on the basis of cation distribution. From the literature survey, it is observed that Li^+ ions occupy only B-site whereas Co^{2+} ions can occupy both A and B sites [27]. It is also reported that the magnetic moment of Co^{2+} ions is more (3 μ_B) [28] than that of the Li^+ (0 μ_B i.e. non magnetic ion) and is less than that of Fe^{3+} ion (5 μ_B) [29]. By increasing the cobalt substitution in the Li–Co ferrite system, lithium ions may be replaced by the cobalt ions and iron ions so as to increase the resultant magnetization values but in case of pure cobalt ferrites these cobalt ions replace the iron ions that led to decrease in magnetization. As saturation magnetization got increased, the superexchange interaction in the particles between the octahedral and tetrahedral sites also increases with increase in cobalt content in lithium ferrites.

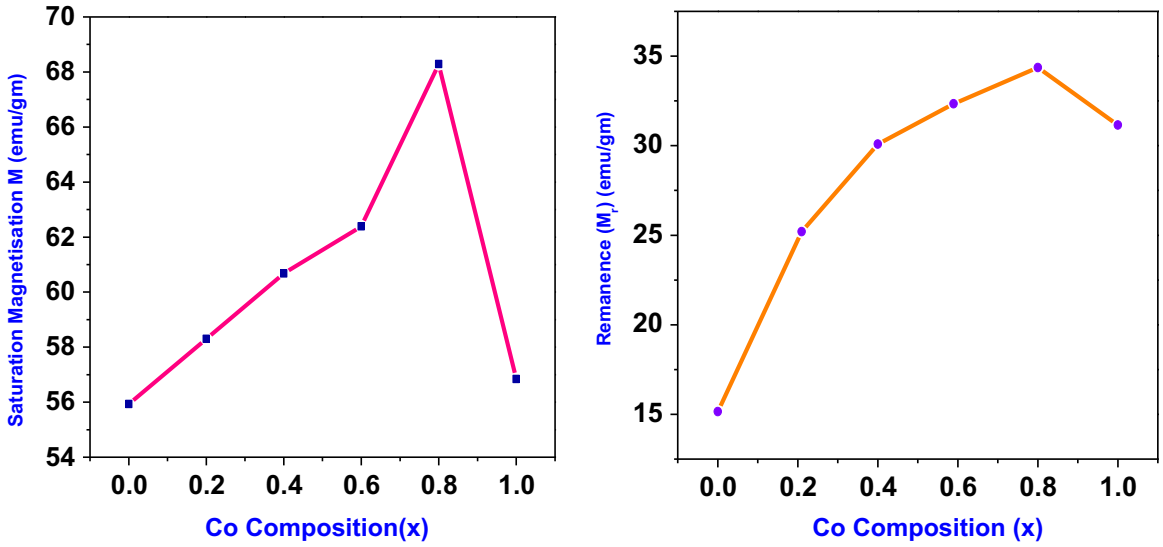

Fig. 4. Compositional variation of Saturation Magnetization (M_s) and Remanence magnetization (M_r) for Li–Co ferrites.

Coercivity is the magnetic field strength required for overcoming anisotropy to flip the magnetic moment which is influenced by the doping of metal ions [30]. The coercivity values were in the range of 153–2099 Oe as clear from Table 2. The magnetic coercivity the materials depends on the magneto-crystalline anisotropic energy, micro-strain, inter-particle interaction, temperature size etc [31]. In cobalt ferrites, the Co^{2+} ($3d^7$, $4F_{9/2}$, $L=3$,$S=3/2$,$J=9/2$) cations possess 7 D-electrons, three of which are unpaired. Evidently, large magneto crystalline anisotropic energy may be due to the strong L–S coupling on the Co^{2+} cation sites. Energy barriers in the individual constituents was considered and introduced by the magneto crystalline anisotropic energy of the prepared cobalt ferrite [32].

The magnetic moment (m) and anisotropic constant (K) of all the Li–Co ferrites were calculated using the relations (4) and (5) from the saturation magnetization (M_s) and coercivity (H_c). The ratio of M_r to M_s, called as squareness ratio or remanence ratio was calculated and all the values are given in the Table 2. From the values, one can observe that the magnetic moment and squareness ratio are observed to be increasing with the increase in the cobalt concentration in Li–Co ferrites.

From all these results, it is apparent that by increasing the cobalt concentration in the nano crystalline Li–Co ferrite, magnetic property of the ferrite samples were improved and the material is being converted from soft magnetic to hard magnetic. Such materials can be used for the fabrication of hard permanent magnets. It is observed that the magnetization values for Li–Co ferrites synthesized by citrate-gel auto-combustion method were higher than those obtained by standard ceramic method [33].

3.4. Electrical measurements

The dielectric constant (ε') and loss tangent ($\tan\delta$) of all prepared samples at room temperature in the frequency range 20 Hz to 2 MHz were measured using LCR meter with the help of relations (6) and (7). The variation of real part of dielectric constant (ε') with frequency was shown in Fig. 5 from which it is clear that the value of ε' decreases with increase in the frequency for all prepared samples, the imaginary part also shows the same variation with frequency (not shown).

Thus, it shows a normal dielectric behavior with frequency. This dielectric dispersion can be explained on the basis of Koop's two layer model [34] and Maxwell-Wagner polarization theory [35–36]. The large value of dielectric constant at low frequency was due to the combined effect of interfacial and dipolar polarizations. With increase in the frequency the dielectric constant decreases, because after certain frequency, the hopping frequency no longer follows the frequency of the applied field. From the Fig. (4), it was observed that pure Lithium ferrites and pure Cobalt ferrites have less dielectric constant values compared with that of substituted Li–Co ferrites. This is because, the probability of hopping of charge carriers between the ions in mixed ferrites was more compared to that in pure ferrites. The variation of dielectric loss tangent with frequency was shown in Fig. 6. In low frequency region, where the high resistive grain boundaries are more effective, more energy is required for electron exchange between the Fe^{2+} and Fe^{3+} ions as a result the loss is high. Whereas less resistive grains are active in high frequency region and less energy is needed for hopping. Hence, loss decreases with increase in frequency [37].

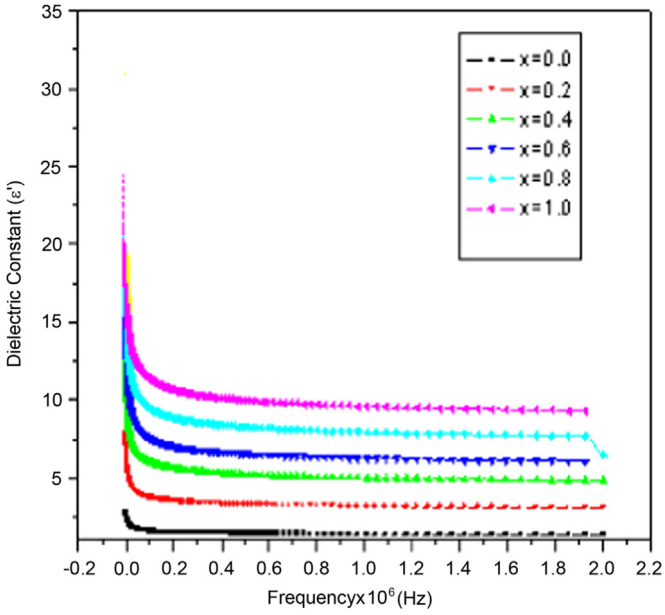

Fig. 5. Variation dielectric constant (ε') with frequency of Li–Co nano ferrites.

The variation of dielectric constant (ε') with cobalt composition is shown in Fig. 7.

From the figure, one can observe that pure lithium ferrites and

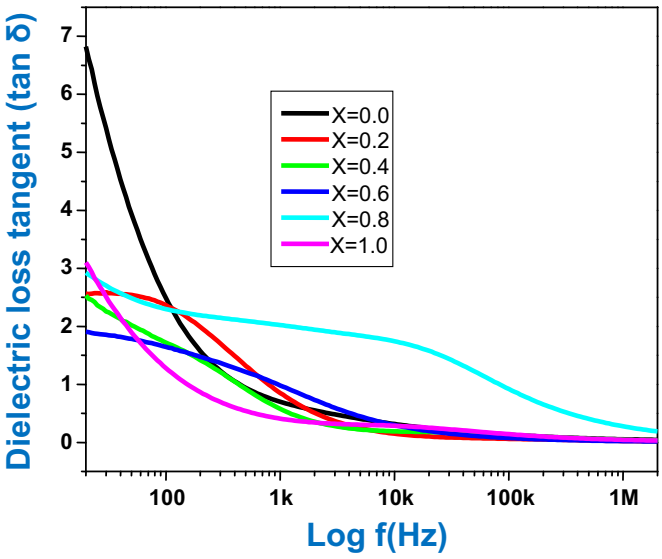

Fig. 6. Variation dielectric loss tangent with frequency of Li–Co nano ferrites.

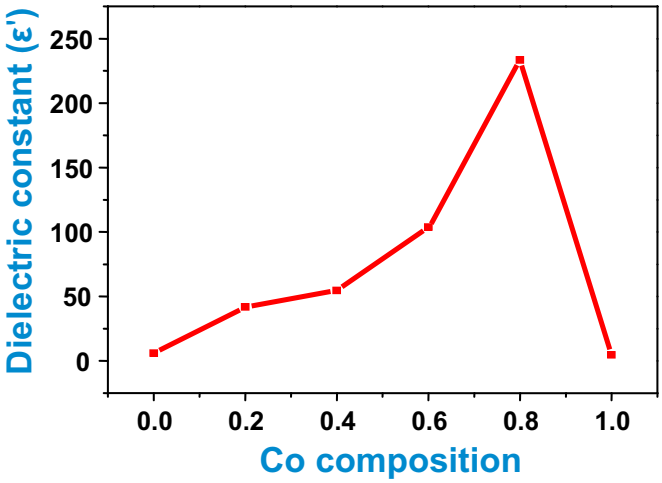

Fig. 7. Variation of dielectric constant with Co composition.

pure cobalt ferrites have less dielectric constant (ε') compared with that of mixed (Li–Co) ferrites. This is because, in mixed ferrites there are more number of charge carriers to increase the polarization effect.

4. Conclusions

Cobalt substituted Lithium ferrites synthesized by auto-combustion method are new materials for the fabrication of hard magnets which is evident from its increased saturation magnetization. The samples prepared were crystalline in nature confirmed by XRD analysis. The crystallite size of the samples was in the range of 36–43 nm. The particles are spherical I shape as studied by FESEM. By increasing the cobalt concentration in the lithium ferrites, the saturation magnetization increased up to $x \leq 0.8$ beyond which it decreased. This is because, Co^{2+} ion with high magnetic moment replaced the non-magnetic Li^{+} ion in the prepared Li–Co ferrite samples. But, in case of pure cobalt ferrites, Co^{2+} ions replaced the Fe^{2+} ions only resulting in decrease in magnetization of pure cobalt ferrite. By increasing the cobalt doping in Li–Co ferrites, the material converted from soft to hard magnetic material. The dielectric parameters of the prepared samples decreased with increasing frequency.

Acknowledgment

The authors are very grateful to Prof. R. Sayanna, Head, Department of Physics, University College of Science, Osmania University, Hyderabad. The authors are also very thankful to UGC, New Delhi, India (Grant Number: F.No. 41-939/2012) for their financial assistance through Major Research Project (M.R.P).

References

[1] M. Raghasudha, D. Ravinder, P. Veerasomaiah, Investigation of superparamagnetism in $MgCr_{0.9}Fe_{1.1}O_4$ nano ferrites synthesized by citrate-gel method, J. Magn. Magn .Mater. 355 (2014) 210–214.
[2] A.K.M. Akther Hussain, M. Seki, T. Kawai, H. Tabala, Colossal magnetoresistance in spinel type Zn_{1-x} $Ni_xFe_2O_4$, J. Appl. Phys. 96 (2004) 1273–1275.
[3] M.A. Ei Hiti, A.I. Ei Shora, S.M. Hammad, Some physical properties of Mg–Zn ferrites, Mater. Sci. Technol. 13 (1997) 625–630.
[4] B.K. Kuanr, Effect of the strong relaxor cobalt on the parallel and perpendicular pumping spin-wave instability threshold of LiTi ferrites, J. Magn. Magn. Mater. 163 (1996) 164–172.
[5] S.C. Watawe, B.D. Sarwade, S.S. Bellad, B.D. Sutar, B.K. Chougule, Microstructure, frequency and temperature-dependent dielectric properties of cobalt-substituted lithium ferrites, J. Magn. Magn. Mater. 214 (1–2) (2000) 55–60.
[6] Mathew George, Swapnw S. Nair, Asha Mary John, P.A. Joy, M. R. Anantharaman, Structural, magnetic and electrical properties of the sol–gel prepared $Li_{0.5}Fe_{2.5}O_4$ fine particles, J. Phys. D: Appl. Phys. 39 (2006) 900–910.
[7] M.U. Rana, T. Abbas, AC susceptibility abd magnetic interaction in Mg–Ni–Fe–O sysem, Mater. Lett. 57 (2002) 925–928.
[8] Qi Chen, A.J. Rondinone, B.C. Chakoumakos, Z.J. Zhang, Synthesis of superparamagnetic $MgFe_2O_4$ nanoparticles by coprecipitation, J. Magn. Magn. Mater. 194 (1999) 1–7.
[9] M.E. Rabanal, A. Várez, B. Levenfeld, J.M. Torralba, Magnetic properties of Mg-ferrite after milling process, J. Mater. Process. Technol. 143 (2003) 470–474.
[10] T. Sasaki, S. Ohara, T. Naka, J. Vejpravova, V. Sechovsky, M. Umetsu, S. Takami, B. Jeyadevan, T. Adschiri, Continuous synthesis of fine $MgFe_2O_4$ nanoparticles by supercritical hydrothermal reaction, J. Supercrit. Fluids 53 (2010) 92–94.
[11] E.J. Choi, Y. Ahn, S. Kim, D.H. An, K.U. Kang, B.G. Lee, K.S. Baek, H.N. Oak, Superpparamagnetic relaxation in $CoFe_2O_4$ nanoparticles, J. Magn. Magn. Mater. 262 (2003) L198–L202.
[12] A. Pradeep, C. Thangasamy, G. Chandrasekaran, Synthesis, structural studies on $Ni_{0.5+x}Zn_{0.5}Cu_xFe_2O_4$, J. Mater. Sci.: Mater. Electron. 15 (2004) 797–802.
[13] B.P. Jacob, S. Thankachan, S. Xavier, E.M. Mohammed, Dielectric behavior and AC conductivity of Tb^{3+} doped $Ni_{0.4}Zn_{0.6}Fe_2O_4$ nanoparticles, J. Alloy. Compd. 541 (2012) 29–35.
[14] A. Verma, T.C. Goel, R.G. Mendiratta, P. Kishan, Magnetic properties of nickel–zinc ferrites prepared by the citrate precursor method, J. Magn. Magn. Mater. 208 (2000) 13–19.
[15] K.V. Manukyan, Y.S. Chen, S. Rouvimov, Peng Li, Xiang Li, Sining Dong, Xinyu Liu, J.K. Furdyna, Alexei Orlov, G.H. Bernstein, W. Porod, S. Roslyakov, A. S. Mukasyan, Ultrasmall α-Fe_2O_3 superparamagnetic nanoparticles with high magnetization prepared by template-assisted combustion process, J. Phys. Chem. C 118 (29) (2014) 16264–16271.
[16] S.A. Saafan, S.T. Assar, B.M. Moharram, M.K. El Nimr, Comparison study of some structural and magnetic properties of nano-structured and bulk Li–Ni–Zn ferrite samples, J. Magn. Magn. Mater. 322 (2010) 628–632.
[17] Mamata Maisnam, Sumitra Phanjoubam, Frequency dependence of electrical and magnetic properties of Li–Ni–Mn–Co ferrites, Solid State Commun. 152 (2012) 320–323.
[18] G. Aravind, D. Ravinder, Preparation and structural properties of aluminium substituted lithium nano ferrites by citrate-gel auto combustion method, Int. J. Eng. Res. Appl. 3 (2013) 1414–1421.
[19] G. Aravind, D. Ravinder, V. Nathanial, Structural and electrical properties of Li–Ni nanoferrites synthesised by citrate gel auto-combustion method, Phys. Res. Int. 2014 (2014), Article ID 672739, 11 pages.
[20] I. Soibam, S. Phanjoubam, C. Prakash, Mössbauer and magnetic studies of cobalt substituted lithium zinc ferrites prepared by citrate precursor method, J. Alloy. Compd. 475 (2009) 328–331.
[21] I.H. Gul, A.Z. Abbasi, F. Amin, M. Anis-ur Rehman, A. Maqsood, Structural, magnetic and electrical properties of $Co_{1-x}Zn_xFe_2O_4$ synthesized by co-precipitation method, J. Magn. Magn. Mater. 311 (2007) 494–499.
[22] H. Yao, K. Kimura, Field emission scanning electron microscopy for structural characterization of 3D gold nanoparticle superlattices, Mod. Res. Educ. Top. Microsc. 2 (2007) 568–575.
[23] M.A. Gabal, Magnetic properties of NiCuZn ferrite nanoparticles synthesized using egg-white, Mater. Res. Bull. 45 (2010) 589–593.
[24] R.C. Kambale, K.M. Song, Y.S. Koo, N. Hur, Low temperature synthesis of

nanocrystalline Dy^{3+} doped cobalt ferrite: structural and magnetic properties, J. Appl. Phys. 110 (2011) 053910–053910-7.
[25] M.M. Hessien, Synthesis and characterization of lithium ferrite by oxalate precursor route, J. Magn. Magn. Mater. 320 (2008) 2800–2807.
[26] M. Ghobeiti-Hasab, Z. Shariati, Magnetic properties of Sr-ferrite nano-powder synthesized by sol–gel auto-combustion method, Int. J. Chem. Mol. Mater. Met. Eng. 8 (2014) 1095–1098.
[27] I. Soibam, S. Phanjoubam, C. Prakash, Magnetic and Mossbauer studies of Ni substituted Li–Zn ferrite, J. Magn. Magn. Mater. 321 (2009) 2779–2782.
[28] S.T. Assar, H.F. Abosheiasha, Structure and magnetic properties of Co–Ni–Li ferrites synthesized by citrate precursor method, J. Magn. Magn. Mater. 324 (2012) 3846–3852.
[29] N. Singh, A. Agarwal, S. Sanghi, P. Singh, Synthesis, microstructure, dielectric and magnetic properties of Cu substituted Ni–Li ferrites, J. Magn. Magn. Mater. 323 (2011) 486–492.
[30] M. Raghasudha, D. Ravinder, P. Veerasomaiah, Magnetic properties of Cr substituted Co- ferrite nano particles synthesized by citrate gel auto combustion method, J. Nanostruct. Chem. 3 (2013) 63.
[31] Q. Zeng, I. Baker, V. Mc Creary, Zh Yan, Soft ferromagnetism in nanostructured mechanical alloying FeCo-based powders, J. Magn. Magn. Mater. 318 (2007) 28–38.
[32] M. Georgescu, J. Viota, M. Klokkenburg, B. Enre, D. Vanmaekelbergh, P. Zeijlmansvan emmichoven, Short-range magnetic order in two-dimensional cobalt-ferrite nanoparticle assemblies, Phys. Rev. B 77 (2008) 024423.
[33] S.C. Watawe, B.D. Sarwade, S.S. Bellad, B.D. Sutar, B.K. Chaugule, Microstructure and magnetic properties of Li-Co ferrites, Mater. Chem. Phys. 65 (2000) 173–177.
[34] Erum parvez, I.H. Gul, Enhancement of electrical properties due to Cr^{3+} substitution in Co-ferrite nanoparticles synthesized by two chemical techniques, J. Magn. Magn. Mater. 324 (2012) 3695–3703.
[35] C.G. Koops, On the dispersion of resistivity and dielectric constant of some semiconductors at audiofrequencies, Phys. Res. 83 (1951) 121–124.
[36] J.C. Maxwell, A Treatise on Electricity and Magnetism, Clarendon Press, Oxford (1982), p. 328.
[37] K.W. Wagner, The theory of heterogeneous dielectric, Ann. Phys. 40 (1913) 817–855.